Fracture mechanics in retrospect in contrast to multiscaling in prospect

G. C. Sih[ab*]

[a]*School of Mechanical Engineering, East China University of Science and Technology, Shanghai 200237, China*
[b]*Department of Mechanical Engineering and Mechanics, Lehigh University, Bethlehem PA 18015, USA*

Abstract.

Failure of man-made structures and machine components becomes eminent when they exceed their useful life. Such incidents, however, can be annoying and costly when they involve substantial financial loss and human lives. The post World War II period was an era when large size structures such as passenger air transports, ships, storage tanks, pipelines, etc, were fracturing unexpectedly for no obvious reasons at the time. Crashing of jet transports alerted the FAA to withdraw certification, pipelines failed by rapid crack propagation for kilometers and oil tankers splitted in two were certainly indicative of the lack of fundamental understanding of how to built fail-safe structures. In retrospect, it can be said that the traditional approach of material testing of the 18th century was inadequate for the design and fabrication of large size structures with high constraint and/or high strength metal alloys. New approaches were needed to determine the conditions when material, geometry and loading rate could combine into a state of "brittleness" where a structure can fail with explosion-like speed and no warning. The feeling was that crack-like defects had to be considered as a potential source of failure initiation.

Considerable efforts were initiated to test materials with pre-inserted cracks under different geometries, temperatures, moistures, etc. all of which seem to affect the failure behavior. A major source of unpredictability was contributed by the lack of standardizing and qualifying material by strength and fracture toughness, a new parameter introduced in the 1960s. A knowledge of the trade off between strength and toughness made substantial progress in design against brittle fracture. As energy generation technology advances, it was not long that high temperature resistance ceramics and metal reinforced composites were in demand and started to replace metal alloys. Material anisotropy and nonhomogeneity became a challenge for applying the basic concept of fracture toughness that was restricted to the assumption of material isotropy and homogeneity. Deviations from the homogeneity still leaves the investigators in bewilderment even after more than one half of a century There is a definite reluctance to do away with a discipline that has outlived its usefulness. This trend has no doubt hindered the progress of understanding material behavior at the smaller size and accelerated time scale. The emergence of electronic age with computer related products has no doubt brought new challenges that are unfamiliar to the material scientists and mechanists who can no longer be satisfied just to fiddle at the macroscopic scale alone with equilibrium theories and closed thermodynamic systems.

When specimens are reduced in size to microns and materials are being made by arranging atoms by atoms, the proposition of using the same fracture mechanics approach of the 1960s may raise eyebrows. Apparent fracture toughness obtained from indentation tests of mm in size nano-composite specimens made from zirconia matrix and silicon carbide reinforced by nano particles are typical examples where the test data have little meaning unless the physics of relating microscopic entities to damage resistance parameters are better understood. There may be energy dissipation mechanisms at the lower scale that need to be considered. Electronic imperfections already known to the solid state physicists might have to be considered in models that address mechanical failure. At the atomic scale level, the term hole is meant to describe electron energy plus phonon energy that result in an empty energy state while exciton has been named as excited electron plus hole. Even for the case of a moving crack, gradual build up of phonon emission has been found at the tip associated with dislocation emission and branching. These energy dissipation mechanisms may not be important to very large specimens but they can be significant when specimen size tends to become smaller and smaller. The added conceptual difficulty in extending the size scale of material characterization can also be contributed to the contrasting views of the continuum and particulate. The former has been adopted in fracture mechanics where the average bulk properties of the material are used while the latter focuses

* Corresponding Author: Email: gcs@ecust.edu.cn (G. C. Sih); Fax: 86(21)6425 3500

attention on the movement of the atoms and sub-atomic particles. The reconciliation of these two contrasting view points is not within sight and may represent the stumbling block to connecting macroscopic and microscopic results envisioned by those in the field.

The present trend of industrial development seems to favor the development of theories and test methodologies that can transfer or relate the experience and know-how available at the macroscopic scale to those at the micro- and nano-scales. Regardless of whether such an expectation is realistic or not, the methodology has to be validated one way or the other. To this end, the term "multiscaling" will be used to denote the characterization of material behavior that entails specimen sizes from centimeters to nanometers. It is prudent therefore to learn from past experience those potential approaches that are likely to succeed and those should be cast aside on fundamental grounds. Since hindsight is less challenging than foresight, it is not difficult to find faults associated with theories involving plasticity, strain gradient (identified classically with the Cosserats), damage theory of Kachanov or the alike. There exists no quick remedy for the apparent drawbacks in the development of the continuum mechanics theories. The well known size effect by letting the continuum element size to vanish in the limit has persisted even at recent times. Such an idealization obviously must be overcome or supplemented with additional conditions to address size scales at the micro- and nano-scales.

As an illustration, the dual scale model of a macro-crack and micro-notch defect will be presented to show how the size scale can be extended by three to four orders of magnitude for a crack with opening displacements at both the macroscopic and microscopic scales. Within the same formulation, a model is developed to capture the macroscopic crack tip and the microscopic notch tip stress fields characteristics at the same time. That is the defects at the two different scales can interact. One would influence the other depending on the loading, material and geometry. These findings are based on the volume energy density function. Presumably, scale invariant criterion may be used to connect the results of several dual scale material damage models such that the macroscopic data can be shifted to smaller scales in steps in view of the lack of a theory that can shift the scales from macro to nano in one breadth.

This work is not intended to solve the problems related to material and structure failure of the 21st century, but rather to illustrate the need to seek for new ideas and previously untried methodologies. Confronted in particular is the spatial and temporal changes that have exceeded beyond the range of previous experience. One of the outstanding problems in micro-electro-mechanical devices is associated with the dormancy of devices containing moving parts. Once they are stopped, they remain dormant and would not restart. Apparently, the transfer of the damping force from large moving parts to smaller moving parts do not follow the classical notion of friction which by in large was conceived from the rigid body mechanics. The definition of the friction force relation to normal force being independent of the surface area is an example. When a body is reduced in size, its surface to volume ratio tends to increase rapidly. This effect must be account for by appealing to the basic laws of physics with emphases placed on scale change. At the atomic scale, all disciplines presently referred to as physics, chemistry, mechanics, biology and others would meet on a common ground. The beginning of such a change may start with mesofracture mechanics in place of fracture mechanics.

Keywords: *Multiscaling Damage; Scale Shifting Criterion; Spatial and Temporal Changes; Nano-size Imperfections; Electrons and Phonons; Miniaturized Specimen Testing; Continuum and Particulate; Dual Scale Damage Model; Volume Energy Density; Anisotropy and Non-homogeneity; and Mesofracture Mechanics.*

1. Introduction.

Nearly four decades ago, the first International Conference of Fracture (ICF) was held in 1965 at Sendai, Japan. The meeting was spear-headed by the authorities of those in the field of dislocation theories. One of the expectations was to connect the atomic dislocation model with the continuum model of fracture mechanics. As time went on and the Pandora box of fracture mechanics opened wider and wider, it became clear that the process of material damage is far more complex than it was envisioned in 1965. While high power resolution election microscopes continue to supply detail features of the material structure at lower and lower scale level, they did not seem to enhance the understanding how defects at the atomic scale led to failure at the macroscopic or structure scale level.

Arbitrary scale divisions were defined to record data more than necessary. Refinement of the divisions were thought to be the missing link in unraveling the source of failure initiation.. Since there is no end to this process of closing the gap, a mesoscopic range had to be admitted as a matter of necessity and a reminder that there might be permanent gaps between the macroscopic and microscopic scale levels. .As technology development would not wait for the development of theories in science, nanostructure materials fumbled into industrial applications by the beginning of the 21^{th} century. Microstructure effects are still far from being understood in connection with their changes on macroscopic material properties.

While the origin of failure will probably never be found, neither will the advancement of science and technology follow an orderly sequence. The trend of learning "what is not" rather than 'what should be" will continue. This is certainly true for the dislocation theories which were thought to be the source of failure initiation for decades until the discoveries that electron defects can also affect the material behavior [1,2]. Even the existence of the basic building block of matter is being seriously questioned as particle physics has found its limitation when the size scale is made smaller and the action of time became so much faster.

In view of what has been said, it would be naïve to still consider fracture mechanics as a technology developed from science. Certainly, the discipline is not to understand the fundamentals of why and how a material would fail but rather to develop a set of guidelines for the industry to apply in order to minimize inconsistencies that would cause social unrest. This can be evidenced in the FAA guidelines for certifying aircraft structural components and sub-assemblies, NRC regulations for nuclear reactor components [3,4] (ASME Codes Section III and XI), welding codes for ship structure, etc. This procedure, however, will obviously lead to chaos since the intent is not to resolve the real technical problem of failure but rather to control the fabrication of commercial products. The wealth from industrialization benefited the developed countries at a much faster rate than that of the undeveloped countries although the truth was often hidden from the public. The priorities of how to use the resources of each country differ widely and they might be far more relevant than the application of codes and standards that were fostered by the developed countries via the development of fracture mechanics. It is not likely that the global trend would continue along this path.

The implication of the foregoing remarks cannot be overemphasized with regard to applying the plane strain fracture toughness value K_{1C} concept as endorsed by ASTM for a homogenous material to composite materials that are non-homogeneous and anisotropic. Misapplication of the classical critical energy release rate or stress intensity factor became apparent as they depended on the fiber orientation, stacking sequence and the microstructure of the composite material constituents. The interaction effect of load, geometry and material dependent parameters can no longer be isolated from one another. Ambiguities started to multiply involving the dependency of critical intensity factors on loading type and material microstructures.

Being a tailor-made material for serving a specific mission, it would be futile to standardize composite material testing because this would defeat the purpose of its very own existence. Use specificity and standardization are two opposing ends of the pole. It has been problematic and frustrating to say the least when the designers are forced to use the codes in situations where they are not intended for. Certainly, the empirical guidelines developed for mechanical structures can hardly be used or even considered for electronic devices [5,6] there are many times smaller than the standard ASTM fracture test specimens [7]. It makes little sense to apply data collected from a large specimen as an average to analyze the behavior of a portion of its constituents. What boils down to is that the transfer of test data from smaller specimens to larger structures as practiced in fracture mechanics may not apply is the procedure is now reversed. That is the large specimen data is now be used for smaller specimens in microns. It goes without saying that there are fundamental issues involved why scaling from small to large is not the same as from large to small.

This work will take the opportunity not only to point out the changing time where science and technology will no longer be made available to the community at large but they will be carefully guarded by individual institutions and isolated groups, far from what the process of globalization should be doing. Those professional societies such as ICF, ISM (International Society of Mesomechanics), etc. that are established by the private sectors will have to struggle for their existence if they intend to foster the well being of scientific and technological development of materials and structures. The struggle to control the goal of scientific and technological development

started in the days of Galileo Galilei will continue into the 21st century and beyond.. The technical problems are overwhelmingly difficult as they are without interference from the political and social sectors. Hence, it should not be surprising to learn that many pieces of the puzzle for understanding the material damage process will remain unknown..

In what follows, the discussion may start with scaling, a well known scheme used in aerodynamics where dimensionless groups have been established to transfer parameters measured during wind tunnel tests for the models to the prototypes. The same kind of procedure is applied structural mechanics. Small specimen test data are collected, standardized and used in the design of full scale structures. These ideas relies on the system being homogeneous where the effect contributed by the material is a case in point. The objective is therefore to relate the results of two independent tests: one being relatively simple and the other can be a prototype or a full size structure. The preservation of homogeneity in scale shifting may involve several steps with ratios of 1:4, !:2 and finally 1:1. The first challenge in continuum mechanics is to be able to translate the uniaxial data to the design of a full size structure. Such a possibility was demonstrated [8] for predicting the valid ASTM plane strain fracture toughness value K_{1C} from uniaxial data alone using analytical means. Scaling at the macroscopic scale is needed to minimize the number of tests that might involve different plate thicknesses, different loading rates and different metal alloys [9-11] characterized by the yield strength and fracture toughness value. The three metal alloys commonly used in the 19th/20th century were steel, aluminum and titanium. Macroscopically speaking, their differences can be reflected by the strength and fracture toughness in the initial design stage. At the very minimum, 27 tests would be needed to establish a complete set of design curves where the interactions of load, geometry and material effects can be determined. This may consists of tests for three different plate thicknesses, three for different loading rates and three for different pairs of strength and fracture toughness. Assumed is that a reasonable curve can be drawn from three points. The trick is to be able to linearize the nonlinear data of load versus crack length used in the simplest theory of a single damage parameter, the crack size. Any fracture parameter [12] that would remain non-linear when plotted against the crack length should invariably be disqualified for it is no better than the uniaxial load being non-linear. In this case, the purpose of applying fracture mechanics is being defeated because the discipline was intended to avoid using the non-linear uniaxial strength but a parameter that is associated with the crack length by a linear relation so that data extrapolation can be used to minimize the number of tests.

The concept of scale shifting becomes considerably more sophisticated when the microstructure of the material comes into the picture, i.e., homogeneity is no longer preserved. The degree of homogeneity in a material would change as the size scale is altered from large to small or vice versa. Recent prospects [13-17] of embedding nano-size particles into single-phase or multi-phase materials have generated much interest for elevating the fracture toughness of ceramics which has all of the superior thermal and electrical qualities except for its seemingly brittle behavior. The available techniques for measuring toughness via hardness [13-17], however, require scrutiny as they are based on specimens millimeters in size and smaller. Material constants based on the average bulk properties of the material constants may not be adequate in addition to the difficulties of inserting through cracks in two dimensions for small specimens which are also difficult to secure in load fixtures. The entire procedure and its underlying physical principle of testing macro-size specimens should be thought out in contrast to the testing of specimens micron in size.

Pre-set ideas and fixed notions may not be easily altered, especially when they have been embedded in the mind for sometime. The physical significance of apparent linearity on a stress and strain curve in contrast to a non-linear curve has not been well understood and has been subject to incorrect interpretations. The ordinary notion that linearity is associated with elasticity and non-linearity with plasticity is obviously an oversimplification. Reference should be made to the degree of homogeneity within the test specimen in terms of microstructure entities or defect size and distribution. If homogeneity is associated with linearity, then non-homogeneity would be related to non-linearity. A consistent scheme in the scaling of size and time can be devised to address the problem of multiscaling [18].

Recognizing that continuum mechanics is divorced from addressing size effect and material damage, numerous attempts have been made to overcome these shortcomings in the 20th century with little or no success. The axioms in continuum mechanics by in large are borne from the motion of particles that seem to describe the behavior of celestial bodies sufficiently well but they leave much to be desired for

deformable bodies. They rely too heavily on notions borrowed from rigid body mechanics where the mutual interaction of the surface and volume is completely ignored by invoking the concept of a closed thermodynamic system where the conditions on the surface or interface need not be determined but are assumed. They are now known as boundary value problems [19,20]. This departure from reality has divided mechanics and material science, the separation of which has stymied the progress in both fields. Such a consequence can be realized from the application of toughness concept to characterize materials reinforced by nano-size particles [13-17]. Possibly a middle ground can be found for the reconciliation of the two disciplines. This is in part the objective of this work for introducing a multiscaling model that can be spared from the overly idealized assumptions of classical mechanics and yet it contains sufficient rigor to capture the reality of non-homogeneity of the material microstructure when viewed at the different scales. For the lack of a better approach, the singularity representation method [18] will be endorsed to illustrate that the scaling of non-homogeneous systems can be addressed in steps by a relatively simple model based on dual scaling.

2. What is there to gain in fracture mechanics that classical failure criteria cannot do?

The replacement of classical failure theories by fracture mechanics was initiated after World War II when Boeing [21] recognized that special attention had to be given to the presence of an initial flaw in the material. Under highly constrained conditions, a small flaw in the form of a crack can grow and reach a critical size to trigger instability of the structure. Such a condition cannot be allowed in the design of a jet airliner which is internally pressurized, a situation that is new to the designer at the time. Panels of different thicknesses and aluminum alloys prepared with artificially inserted cracks were tested to fracture for establishing the failure envelop that divided the combination of stress and crack length that would or would not lead to fracture. For monolithic structures, it was soon recognized that a damage length parameter should enter into the design criterion. When this is done, the scattered of the SN-curves for fatigue were drastically reduced, an indication of improvement in data collection. It was not long, a consortium consisting of the Boeing Transport Division, the Structural Branch of the US Naval Research Laboratory and the Department of Mechanics at Lehigh university [22] was formed and funded to investigate the remaining strength of materials and structural components with initial cracks under different load and moisture conditions. The interaction of these three groups of researchers and engineers was the start of a learning process that has led to the application of fracture mechanics to other fields such as ship building, nuclear vessel construction, pipeline fabrication, rail inspection, just to mention a few.

2.1 Linearization of crack length test data.

Linear extrapolation of test data is pertinent in design for it can minimize the number of tests and save cost. To use the material or structural component response beyond the linear range, it meant that tests have to be performed for all conceivable geometries and loadings. This renders the procedure unviable. What is needed is to seek for a fracture mechanics parameter that would linearize the non-linear load versus crack length data, if possible [23]. Suppose that geometry, material and loading rate were chosen as the primary variables in design. Let the geometry effect be represented by the panel thickness of thin, moderate and thick, the loading rate by slow, medium and fast while the materials by aluminum, steel and titanium characterized by their strength as being soft, medium and hard together with their fracture toughness values. Assuming that three points suffice to draw a curve, this would require a minimum of 27 tests for a complete set of design data where the effects of geometry, loading rate and choice of material are taken into account.

2.2 Specimen with geometric similarity.

To illustrate what has been mentioned, consider a panel with thickness h, width 2c and height 2b that contains a central crack of length 2a. Uniform stress of magnitude σ_∞ normal to the crack is applied on the panel outer edge. The objective is to use a fracture parameter, namely the strain energy density factor S [24] and to show that straight line relationships are obtained when S is plotted against the critical crack length at incipient rapid fracture. Three different loading steps of $\Delta\sigma$ equal to 155.14, 189.61 and 241.33 MPa and three different materials will also be selected [24]. Refer to Tables 1 and 2

in which V/A stands for the volume to surface area of the panel and σ_{ys} and σ_{ul} are, respectively, the yield and ultimate strength of the material. Note that $(dW/dV)_c$ represents the critical area under the true stress and strain curve where the terminal stress corresponds to the ultimate stress σ_{ul}.

Table 1. Geometrically similar center-cracked panels.

Specimen Type	Dimensions(cm)				
	V/A	a	b	c	h
I	1.105	2.54	25.40	12.70	2.54
II	2.031	7.62	76.20	38.10	7.62
III	2.931	17.78	177.80	88.90	17.78

Table 2. Three different metal alloys.

Material type	σ_{ys} (MPa)	σ_{ul} (MPa)	$(dW/dV)_c$ (MPa)	$(dW/dV)_c^*$ (MPa)
I	620	1,172	4.7	3.3
II	517	1,379	12.3	4.6
III	412	1,586	49.8	6.1

2.3 Stable crack growth criterion.

The strain energy density criterion [9-11] assumes that the nearest element next to the crack tip would break when dW/dV reaches $(dW/dV)_c$. If there are energy loss such as plastic deformation before the incipient of rapid fracture, then the lost portion of the energy density must be subtracted from $(dW/dV)_c$ leaving only the amount that is available to set the crack into rapid motion. This available energy density is denoted by $(dW/dV)_c^*$ which is obviously less than $(dW/dV)_c$ as tabulated in Table 2 for the three different materials.

The incremental theory of plasticity [25] is now applied to solve this crack problem by means of the finite element method [26] for the elastoplastic stresses and strains ahead of the crack while the load σ_o is increased in constant steps of $\Delta\sigma$. The crack is set into motion by having the dW/dV in the nearest element ahead of the crack tip to reach $(dW/dV)_c$ or $(dW/dV)_c^*$. Stable crack growth in steps of r1, r2, etc., are assumed to take place according to

$$(\frac{dW}{dV})_c = \frac{S_1}{r_1} = \frac{S_2}{r_2} = \cdots = \frac{S_j}{r_j} = \cdots = \frac{S_c}{r_c} \tag{1}$$

Unstable fracture is assumed to coincide with satisfaction of the condition:

$$(\frac{dW}{dV})_c = \frac{S_c}{r_c} \tag{2}$$

where r_c is the critical ligament ahead of a crack. The critical strain energy density factor S_c can be view as the energy release by the crack extending the amount r_c. Although the load increment is taken to be constant, the crack may not grow in constant segments. In general, crack growth would follow a combination of

$$r_1 > r_2 > \cdots > r_j > \cdots > r_a,\ S_1 > S_2 > \cdots > S_j > \cdots > S_a \tag{3}$$

and

$$r_1 < r_2 < \cdots < r_j < \cdots < r_a,\ S_1 < S_2 < \cdots < S_j < \cdots < S_a \tag{4}$$

Eqs. (3) represent the decrease of successive crack growth segments while eqs. (4) represent the increase of successive crack growth segments. In general the load can increase and decrease and the crack growth history is likely to be described by the combination of the conditions in eqs. (3) and (4) in which S_a, r_a and S_c, r_c correspond to the crack arrest and rapid crack initiation values of S and r, respectively.

2.4 Linear interpolation.

Computation of the elastoplastic stresses will be made for $\Delta\sigma$ = 241.33 MPa and a material with $(dW/dV)_c$ = 12.31 MPa. The results for the three different V/A values in Table 1 are displayed in Fig. 1 in terms of the variations of the strain energy density factor S with the amount of crack growth r-a. For each value of V/A a straight line was found. A S value of 96 kN/m was obtained for the highest point of the V/A = 6.840cm curve. This finding is significant because parallel lines corresponding to other value of V/A can simply be obtained by linear interpolation of the data. Knowing the critical value of S_c for a given material. A horizontal line can thus be drawn in Fig. 1 to obtain three critical crack length to establish a curve of V/A versus critical crack length. Hence, the threshold conditions for panels with thicknesses other than those tested can be found directly from the graphs. This in essence is the advantage of using the criterion S in contrast to the energy release rate or path independent integral [12].

Now, consider the same material with $(dW/dV)_c$ = 12.31 MPa and set V/A = 1.105cm. The loading steps will be varied as $\Delta\sigma$ = 155.14, 189.61 and 241.33 MPa, another set of three curves will be obtained in a plot of S versus half crack length a. Again, all the curves in Fig. 2 are straight lines but they are no longer parallel. The trend is that they intersect at a common point. A counterclockwise rotation can bring the curve with the smaller load step to those with the larger load steps. Again, linear extrapolation of test data can be used to fill in the spaces where lines for the other load steps would occupy.

The technology for adjusting the yield strength σ_{ys} and fracture toughness K_{1C} of metal alloys is well known. Within the framework of macroscpic fracture mechanics, it suffices to specify σ_{ys} and K_{1C} for determining the type of metal alloy needed in design. By using an appropriate trade off relationship between σ_{ys} and K_{1C}, it is sufficient to specify $(dW/dV)_c^*$ = 3.32, 4.60 and 6.08 MPa as depicted in Table 2. With V/A = 1.105cm and $\Delta\sigma$ = 241.33 MPa, three straight lines intersecting at a common point can be obtained as given in Fig. 3. The horizontal lines represent the critical S. They intersect with the slanted lines labeled by $(dW/dV)_c^*$ and determines the critical crack lengths.

2.5 Physical meaning of the S-curves.

Summarized in Figs. 4(a), 4(b) and 4(c) are respectively, the crack growth resistance or S-curves to account for changes in specimen size, loading rate and material toughness. The data in Figs. 4(a) and 4 (b) are obtained for a given material. Hence, a single horizontal line representing S_c prevails for finding the critical crack lengths. Three horizontal lines, one for each of three materials, appear in Fig.4(c) for obtaining the critical crack sizes. The following interpretations can be made from the S-curves in Figs. 4(a) to 4(c).

- Fig. 4(a) – As the specimen size increase with the V/A ratio, the critical crack size decreases. Small critical crack size corresponds to “brittle” fracture while large critical crack correspond to ductile fracture. The interim stages stand for failure by the combination of yielding and fracture where subcritical crack growth precedes the onset of rapid fracture.
- Fig. 4(b) – The slopes of the curves increases with increasing loading rates. Small load steps therefore tend to enhance stable crack growth and delay the onset of rapid fracture while large load steps would favor sudden fracture. The S-curves for varying loading rate can be used in accelerating time tests where short time to failure test data can be related long time failure test data.
- Fig. 4(c) – Construction of the S-curves with appropriate trade off properties in strength and fracture toughness provides the methodology for fabricating use-specific materials.

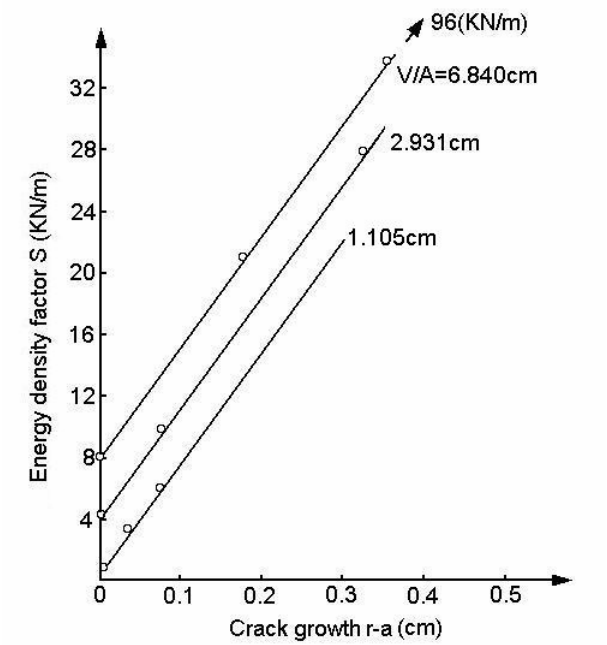

Fig. 1 S-curves for $\Delta\sigma$=241.33MPa and $(dW/dV)_c^*$ =4.6MPa

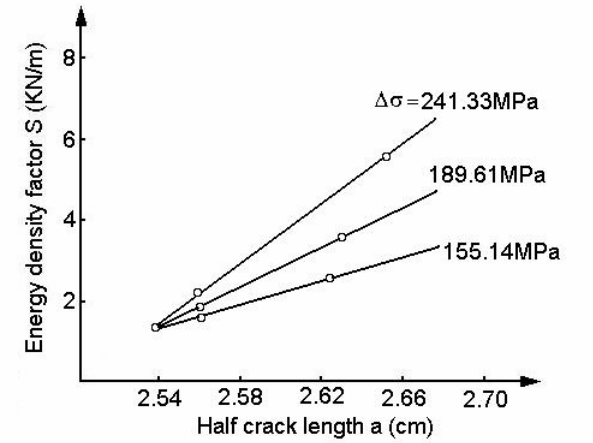

Fig. 2 S-curves for V/A=1.105cm and $(dW/dV)_c^*$ =4.6MPa

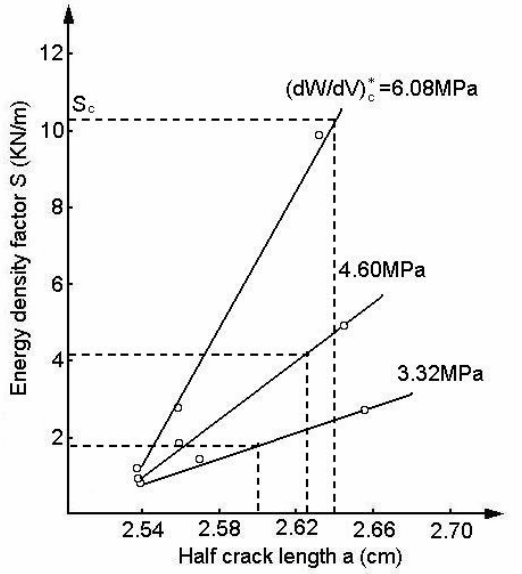

Fig. 3 S-curves for V/A=1.105cm and $\Delta\sigma$=241.33MPa

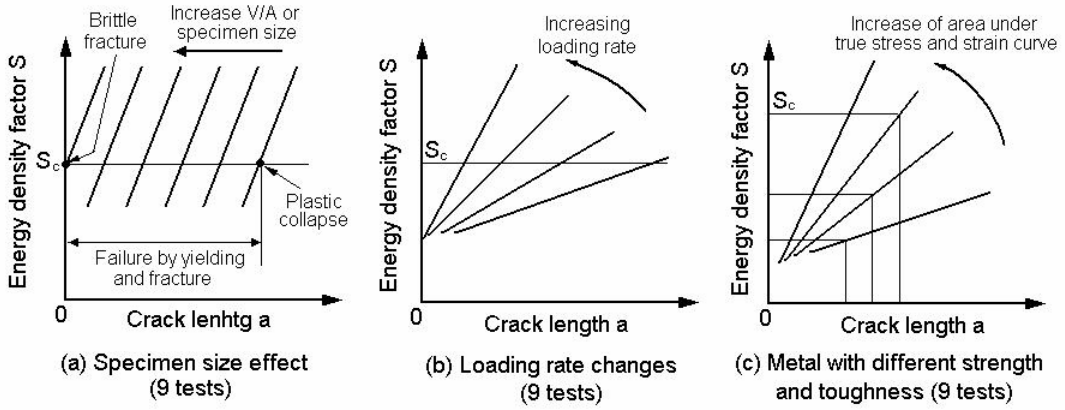

Fig. 4 Minimum of 27 tests to cover variations of specimen size, load rate and material behavior

2.6 Remarks concerning the restrictive nature of macro-fracture model with the upcoming of nanotechnology.

Up to this point, the scale of observation has been assumed to be sufficiently large such that the microstructure details of the material can be averaged out and considered as material constants in the constitutive relations. Such a simplification worked well for high strength polycrystals where their grains are relatively small such that homogeneity can be invoked. The same applies to the design of large structures where their components are comparable to the size of test specimens. When the aforementioned conditions of homogeneity are violated, it becomes necessary to seek for new approaches and models that would address the problem at the grass root level. Non-homogeneity and mutltiscaling are the up-coming challenge in material science and mechanics when the late Richard T. Feynman convinced the technical community that the conservation of energy lies in making machine smaller. His one line calculation of energy used in a transistor was sufficient to illustrate that decrease in size translates into faster speed and less energy. Quote from Feynman's hand calculation:

$$\text{"Energy} \bullet \text{time for transistor} = kT \bullet \frac{\text{Length}}{\text{Thermal vel.}} \bullet \frac{\text{Length}}{\text{Mean free path}} \bullet \text{No. of electrons"}$$

This gives

$$\text{Energy} \cong 10^{9\text{-}11}\ kT \text{ and hence "decrease size: faster \& less energy".}$$

where k is the Boltzmann constant and T is the absolute temperature.

3. Is the fracture toughness concept still valid for micro- or nano-size specimens?

The emergence of nanotechnology has led to a resurgence of interest in the development of materials that can resist high temperature. The calculation of Feynman is indicative of the level of thermal energy in units of kT in a transistor of the future. The candidate materials are the nano-composite ceramics made from zirconia (ZrO_2) matrix and silicon carbide embedded with nano-particles 60nm in diameter. Because of the prohibitively high cost of fabricating nanosize particles, specimen size is limited to millimeters. A typical size would be 36mm×4mm×0.4mm. The reinforced composites can be made by coagulation casting typically with volume fraction of nano-particles up to about 30% while the sintering temperature can be varied from 1,600 to 1,800 ^{o}C. Having established the ground rules, the task of research in material characterizaton is to show whether the addition of nano-particles can indeed enhance the fracture toughness of ceramics which are known to be brittle. The current belief of the toughening mechanism [13,14] has been attributed to the switching of inter- to trans-granular failure by distributing nano-particles along the grain boundary. Surface roughening may also help. The basic thought is prolongation of the crack path. There is the more fundamental question of characterizing the toughness of composite ceramics for specimens that are too small to meet all of the idealized mechanical conditions assumed in the theory of the two-dimensional macro-fracture model. If the crack surface is not aligned normal to the specimen surface and/or loading plane, three-dimensional effects will be involved. Since the surface to volume ratio for small specimens is increased many folds, the fracture model based on the neglect of such effects would yield inaccurate results [27]. These and other potential problems that may have been

overlooked in the current approaches will be discussed.

3.1 Implicitly assumed hardness and toughness relation in test methods.

The macro-fracture model based on LEFM (linear elastic fracture mechanics) ideas relies on the creation of distinct new fracture surface that can be measured at the macroscopic scale. Being a two-dimension model, crack extension in the thickness direction of the plate is assumed to be uniform. Hence, the measurement entails only the extended crack length. Despite the extensive efforts made to extend the LEFM model to material with dissipation and to three-dimensional cracks, the investment has far exceeded the gain in return. This, however, cannot justify the oversimplification of the fracture model. The implications of the two current fracture toughness measurment techniques deserve attention.

Indentation- strength approach. Developed in [15,16] is an empirical relation that expresses the apparent fracture toughness K_C in terms of the inert strength σ_m and Vicker hardness number H as given by

$$K_c = 0.52\left(\frac{E}{H}\right)^{\frac{1}{8}}\left(\sigma_m P^{\frac{1}{3}}\right)^{\frac{3}{4}} \tag{5}$$

where E is the Young's modulus and P the contact load. The form of K_C as given in [15,16] has been rearranged to the form in eq. (5). The symbol K_{1C} is reserved for the ASTM valid plane strain fracture toughness value which should be distinguished from K_C in eq. (5) which may not be entirely related to the creation of new fracture surface. For the Al_2O_3 ceramic, the Young's modulus E = 393 Gpa. If a 5% SiC nano-particles is added (E_{SiC} = 435 MPa), there is hardly any effect on the E for Al_2O_3. Hence, the same E in eq. (5) can be used with or without the nano-particles. Referring to Figs. 5(a) and 5(b), H can be calculated as

$$H(\text{Vicker}) = \frac{2P}{d_o^2}\sin\frac{\alpha}{2},\ \ h_o = \frac{d_o}{7} \tag{6}$$

The opening angle of the indentation $\alpha = 136^o$. Hence, all parameters in eq. (5) can be made known for computing H. The toughness K_C for Al_2O_3 was found [15] to increase from 3.25 to 4.70 MPa·$m^{1/2}$ after adding 5 volume % of 0.3μm SiC particles. A 13.85% increase is not a significant improvement even if K_C were assumed to be representative of fracture toughness.

Indentation-crack length approach. This method also uses the Vicker hardness test set-up in Figs. 5(a) and 5(b). The impact load is large enough such that cracks would extend from the corners of the indentation as illustrated in Fig. 6 where $b_o = d_o + a_o$. Depending on the size of the cracks, two relations for K_C are given in terms of H. They are given by [14,17]:

$$K_c = 0.223E^{2.5}\frac{d_o}{b_o}\frac{1}{\sqrt{b_o H}},\ \text{for}\ \ b_o/d_o > 2.5 \tag{7}$$

and

$$K_c = 0.0606E^{2.5}\sqrt{\frac{d_o}{a_o}}\frac{d_o}{\sqrt{H}},\ \text{for}\ 0.25 < a_o/d_o < 2.50 \tag{8}$$

Nano-particles of SiC and ZrO_2 were added to the Al_2O_3 matrix. Change in the fracture toughness [14] of the composite with the vol. % of ZrO_2 as the sintering temperatures varied from 1,500 to 1,700°C. The K_C values scattered from 4.3 to 6.3. MPa•$m^{1/2}$ depending on the vol. % of ZrO_2.The highest K_C were obtained for composite with sintering temperature of 1,700°C.

Seek for alternatives. It is seen from eqs..(5), (7) and (8) that a trade off relation between fracture toughness and hardness has been assumed. It has been implied that

$$\text{Toughness} \bullet (\text{Hardness})^n = \text{constant} \tag{9}$$

where n in eqs. (5), (7) and (8) differed in value. The obtained data in [14,17] contained too much scatter which may be attributed to the difficulties involved to indent small composite ceramic specimens with consistency. The explanation for the increase in K_C is speculative at best. The destructive methods of strength and toughness testing become overwhelmingly difficult and less reliable as the specimen size is reduced.

To be questioned is whether the fracture mode of failure is realistic for micron size specimens. The

answer is probably “no”. The intensified heat created in a microchip is likely to cause the malfunction of the device. It is illustrated in Fig. 7 that the intensity of the heat flux in a microchip is comparable to that of a nuclear blast. Since the chip is so small, the nano explosion will not be life threatening to human but it is enough to break down a microchip. Simply stated, the primary cause of failure should no longer be focused solely on cracking of the structure as in an aircraft. There are the thermal, electrical, magnetic and other energy sources that can alter the behavior of material micro-structure which changes its degree of inhomogeneity at the different size scales. The criterion of failure should be focused on exceeding certain threshold of energy density in relation to the malfunction of the device in question.

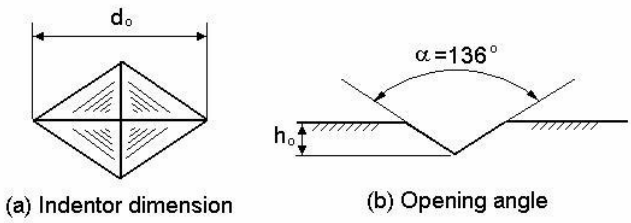

Fig. 5 Vicker hardness indentation test

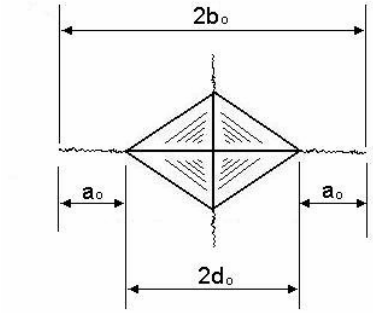

Fig. 6 Cracks radiating from indentor corners

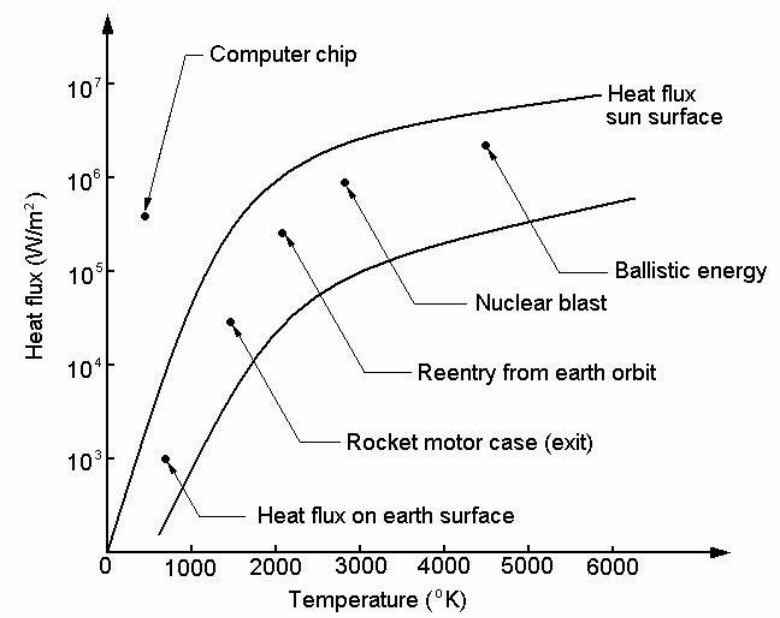

Fig. 7 Heat flux in computer chip comparable to nuclear blast

4. Singularity representation of dual scale model for macro- and micro-defect interaction.

The study of material damage have not progressed as much as it should because of distractions from

the development of continuum mechanics and material science fields that seem to be relevant at the time. The two outstanding misjudgments are concerned with the theories of plasticity and dislocation both of which have not helped fracture mechanics to advance as the fundamental problem of scaling and non-homogeneity remain untouched. Up to now, there is sufficient evidence to realize that any realistic model of material damage should include the feature of multiscaling where the combined changes of geometry, loading and material should be reflected. What this implies is the non-existence of specific intrinsic material constants that could be used without regard to size and the time scales. The notion of the atomic cohesive strength of solids is an oversimplification of reality that has been taken for granted even though experimental works show otherwise. It has been demonstrated in [18] that the state of affairs ahead of a crack at the microscopic scale are still very sensitive to changes in load, geometry and material properties. There is no valid reasons to believe that the changes in geometry, load and material properties would vanish when the scales are reduced. The idea of a constant should not be used in an open ended manner; it should be qualified with the restrictions in terms of size and time scales. The Hubble constant adopted in cosmology needed adjustment after the discovery that the universe [28] was found to be much younger than originally estimated by the Big Bang theory. The chance for finding material constants is much worse when matters are examined at smaller and smaller size scales. The calculations based on using the Thomas-Fermi-Dirac potential [29] show that there are significant differences in the density of the electrons which may be regarded as interface in nano-materials.

4.1 Mesoscopic zone of restrain.

The connection between the macro-crack and the micro-notch is made possible via a mesoscopic zone of length b-d as shown in Fig. 8. The half length of the macro-crack is a while the length the micro-notch is d such that the overall half length of the macro- and micro-defect is c. Reference is made to the Cartesian coordinate system $(x_1,x_{2)}$. The dual scale defect system is subjected to equal and opposite uniform stress σ_o applied at a remote distance from the macro-micro-defect. Modeling of the macro-crack will be distinguished from that of the meso- or micro-defect by the applied tractions. The former will be traction free as defined traditionally while the latter will be subject to surface tractions because the adjoining surfaces of micro-defects would be relatively close and in contact. These contacting stresses will be referred as the restraining stresses that were first used in relation to the problem of a moving crack [30] and later to the singularity representation of a dual scale crack model [18] which is the subject of this discussion. The restraining stress should be distinguished from the cohesive stress concept in other crack problems. It is no longer assumed as an intrinsic material property. The atomic cohesive strength between a pair of atoms is assumed to be unique and independent of the geometry and loading, a proposition that is no longer acceptable in light of what is observable by the high resolution electron microscope. The state of affairs very close to the crack tip in a thinned-down metal have been observed to be extremely sensitive to the applied mechanical loads. This is manifested by the emission of dislocations [31] in several metal alloys.

Returning to Fig. 8, the mesoscopic zone is shown to terminate at the micro-notch modeled by a wedge-shaped re-entrant corner with an angle 2β. At both ends of the mesoscopic zone, the half opening displacements are denoted by δ^* and δ which are referred to, respectively, as the restraining zone opening displacement (RZOD) and the crack opening displacement (COD), Fig. 9. Since the combination of b, d, δ^* and δ changes with the applied load, macro-crack length and micro-notch geometry, they have to be determined for each specific situation. This, in retrospect, points out the likelihood of making potential errors in modeling multiscale crack systems when the coupled interaction between the macro- and micro-defect is not properly accounted for. The challenge is to couple the singular character of the defect stress fields, one at the macroscopic scale and one at the microscopic scale.

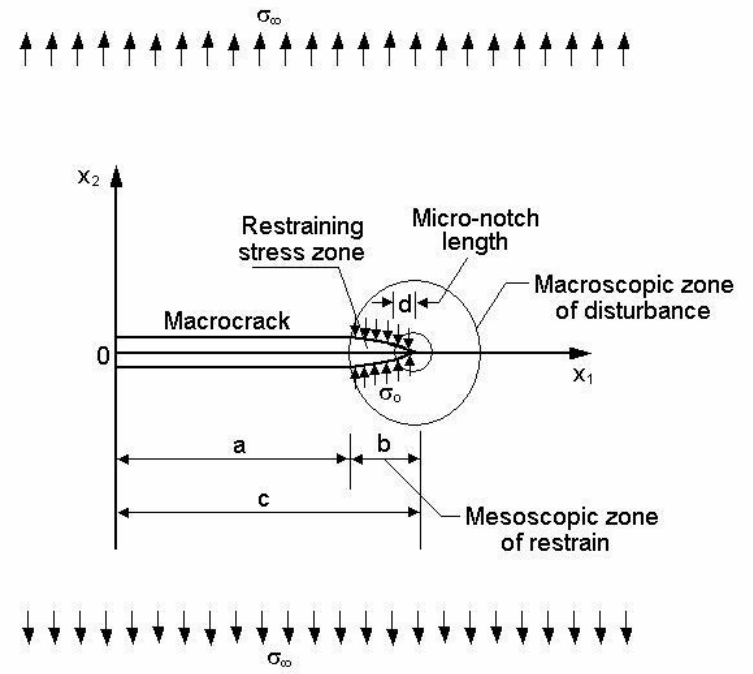

Fig. 8 Schematic of micro-meso-macro- defect system

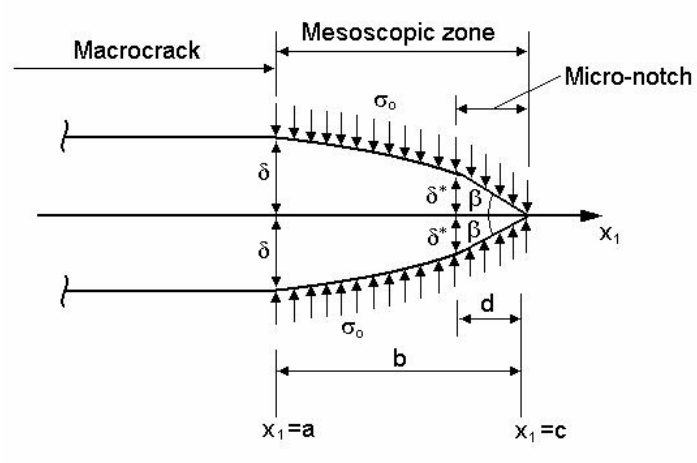

Fig. 9 Enlarge view of micro-notch tip

4.2 Macroscopic and microscopic zone of disturbance.

Illustrated in Fig. 8 is two regions of stress and strain field disturbance. They are localized near the macro-crack and micro-notch tip. Since their intensity and size differ by orders of magnitude, they can be determined separately and then connected by stress and opening displacement compatibility conditions.

Macro-crack singularity. The singular character of the macro-crack tip stress field can be found for the mode I loading situation in Fig. 8. In this case, it suffices to consider one complex function $\Phi(z)$ of the complex variable $z = x_1 + x_2$ for the stress combinations:

$$\sigma_{11} + \sigma_{22} = 2[\Phi(z) + \overline{\Phi(z)}],\ \sigma_{22} - \sigma_{11} + 2i\sigma_{12} = \sigma_\infty - 4ix_2\Phi'(z) \tag{10}$$

and displacement combinations

$$2\mu\frac{\partial}{\partial x_1}(u_1 + iu_2) = (3-4\nu)\Phi(z) - \overline{\Phi(z)} - \frac{1}{2}\sigma_\infty - 2ix_2\overline{\Phi'(z)} \tag{11}$$

where μ is the shear modulus and ν the Poisson's ratio. Near a defect, a state of plane strain always prevail:

$$\sigma_{33} = \nu(\sigma_{11} + \sigma_{22}),\ \sigma_{13} = \sigma_{23} = 0 \tag{12}$$

The boundary conditions for a free surface crack will be used:

$$\sigma_{12} = 0,\ x_2=0;\ \sigma_{22} = 0,\ x_2=0 \text{ and } |x_1| < a \tag{13}$$

where symmetry requires that

$$u_2 = 0,\ \text{for } x_2=0 \text{ and } |x_1| > c \tag{14}$$

Restraining stress σ_o is prescribed along the segment of the mesoscopic zone. This is satified by the condition

$$\sigma_{22} = -\sigma_0,\ \text{for } x_2=0 \text{ and } a < |x_1| < c \tag{15}$$

Finally, the conditions far away are given by

$$\sigma_{22} \to \sigma_\infty,\ \sigma_{11} \to 0,\ \sigma_{12} \to 0,\ \text{for } z \to \infty. \tag{16}$$

which corresponds to the specification of tension applied in the x_2-direction. This corresponds to a Dirichlet problem and the solution can be found in [32]:

$$\Phi(z) = -\frac{1}{4}\sigma_\infty + \frac{i\sigma_0}{2\pi}\ln\frac{a-z}{a+z} + \frac{i\sigma_0}{2\pi}\ln\frac{\sqrt{(c^2-a^2)(c^2-z^2)} + az + c^2}{\sqrt{(c^2-a^2)(c^2-z^2)} - az + c^2} \tag{17}$$

Differentiation gives

$$\Phi'(z) = \frac{i\sigma_0}{2\pi}\frac{-2a}{a^2-z^2} + \frac{i\sigma_0}{2\pi}\frac{2a}{\sqrt{c^2-a^2}(\sqrt{c^2-a^2}+\sqrt{c^2-z^2})} \tag{18}$$

It should be noted in passing that the finiteness condition of the crack tip stresses has been enforced at this point in previous crack models using the argument that infinitely large stresses do not exit on physical grounds. The work in [33] and [34] make use of a cohesion zone and yield zone, respectively, to alienate the singularity at the crack tip. The exclusion of an unbounded stress in fact was understood in the problem formulation when admitting the Plemelj function for describing the crack tip behavior for otherwise the condition r = 0 would have yielded the trivial solution for the displacement field. Here, r is the distance from the crack tip. The correct mathematical interpretation of the singular solution is that the stresses would *tend* to become very large as $r \to 0$ but it never equals to zero, the initial condition used for finding a non-trivial solution. Strictly speaking, the objection against the stresses becoming unbounded is not a valid argument in mathematical physics.

Without going into details, the boundary and symmetry conditions in eqs. (13) to (16) were applied to yield the complex function and its derivative in eqs. (17) and (18). These expressions can then be substituted into eqs.(10) to yield the macro-meso crack tip stresses having a $r^{-1/2}$ singularity and an intensity factor K^t. More specifically, the stresses σ_{11}, σ_{22} and σ_{12} can be expressed as

$$\sigma_{11} = \frac{K^t}{\sqrt{2\pi r}}\cos\frac{\theta}{2}\left(1-\sin\frac{\theta}{2}\sin\frac{3\theta}{2}\right),\ \sigma_{22} = \frac{K^t}{\sqrt{2\pi r}}\cos\frac{\theta}{2}\left(1+\sin\frac{\theta}{2}\sin\frac{3\theta}{2}\right),$$

$$\sigma_{12} = \frac{K^t}{\sqrt{2\pi r}}\sin\frac{\theta}{2}\cos\frac{\theta}{2}\cos\frac{3\theta}{2} \tag{19}$$

where r and θ are polar coordinates measured from the x_1-axis. The intensity factor contains two parts $K^{(1)}$ and $K^{(2)}$. They stand for

$$K^{(1)} = \sigma_\infty\sqrt{\pi c} \tag{20}$$

the stress intensity factor corresponding to the remote uniform tensile stress σ_∞ and

$$K^{(2)} = -\frac{2}{\pi}(\cos^{-1}\frac{a}{c})\sigma_o\sqrt{\pi c} \tag{21}$$

the stress intensity factor produced by the uniform restraining stress σ_o The negative sign in eq. (21) denotes that σ_o exerts restrain on crack opening from the action of σ_∞. Hence, the total stress intensity factor K^t can be written as

$$K^t = K^{(1)} + K^{(2)} = (\sigma_\infty - \frac{2\sigma_o}{\pi}\cos^{-1}\frac{a}{c})\sqrt{\pi c} \tag{22}$$

As mentioned earlier, the condition $K^t = K^{(1)} + K^{(2)} = 0$ was used in [33,34] to derive the length b for the cohesion or yield zone. In what follows, the singularity representive approach will be applied where

$K^t \neq 0$. A notch tip factor similar to that in [35] will be used.

Micro-notch singularity. As r becomes smaller, a microscopic distance will be reached where the influence of the notch tip having a weaker singularity takes control. The corresponding stress field is no longer $r^{-1/2}$ but r^{λ_1-1} where $\lambda_1 < 1$. The singular portion of the micro-stresses has been determined in [35]. It is given by

$$\sigma_{11}^w = \frac{K^w}{\sqrt{2\pi}}\lambda_1 r^{\lambda_1-1}[(2+\lambda_1\cos 2\alpha+\cos 2\lambda_1\alpha)\cos(\lambda_1-1)\theta-(\lambda_1-1)\cos(\lambda_1-3)\theta]$$

$$\sigma_{22}^w = \frac{K^w}{\sqrt{2\pi}}\lambda_1 r^{\lambda_1-1}[(2-\lambda_1\cos 2\alpha-\cos 2\lambda_1\alpha)\cos(\lambda_1-1)\theta+(\lambda_1-1)\cos(\lambda_1-3)\theta]$$

$$\sigma_{12}^w = \frac{K^w}{\sqrt{2\pi}}\lambda_1 r^{\lambda_1-1}[-(\lambda_1\cos 2\alpha+\cos 2\lambda_1\alpha)\sin(\lambda_1-1)\theta+(\lambda_1-1)\sin(\lambda_1-3)\theta] \quad (23)$$

The stress field immediate to the sharp notch tip possesses a weaker stress singularity of the order of r^{λ_1-1} where $0.5 < \lambda_1 < 1$. A schematic of this dual-scale character of the stresses is shown in Fig. 8. It can be shown that

$$K^w = \sigma_o(\pi d)^{1-\lambda_1} \quad (24)$$

It follows that the enforcement of stress compatibility gives a relation for determining the two unknown b (or c since b = c–a) and d. That is

$$K^w = (\pi c)^{0.5-\lambda_1} K^t \quad (25)$$

which can be written out explicitly in the form

$$\frac{a}{c} = \cos\left\{\frac{\pi}{2}\left[\frac{\sigma_\infty}{\sigma_0} - \left(\frac{d}{c}\right)^{1-\lambda_1}\right]\right\} \quad (26)$$

The second relation can be determined from the compatibility of the opening displacements δ and δ* as defined in Fig. 9. This will be done subsequently.

4.3 Opening displacement compatibility.

Recall that the crack opening displacement COD is denoted by 2δ and the restrained zone opening displacement RZOD by $2\delta^*$. For plane strain, the COD can be derived from the displacement expression. The result is

$$\mathrm{COD} = \frac{4(1-\nu^2)\sigma_0}{\pi E}\left[aX - x_1 Y - 2\sqrt{c^2-x_1^2}\left(\cos^{-1}\frac{a}{c} - \frac{\pi\sigma_\infty}{2\sigma_0}\right)\right], \quad -c<x_1<c \quad (27)$$

in which X and Y stand for

$$X = \ln\left|\frac{\sqrt{c^2-\xi^2}+\sqrt{c^2-a^2}}{\sqrt{c^2-\xi^2}-\sqrt{c^2-a^2}}\right|, \quad Y = \ln\left|\frac{a\sqrt{c^2-\xi^2}+\xi\sqrt{c^2-a^2}}{a\sqrt{c^2-\xi^2}-\xi\sqrt{c^2-a^2}}\right| \quad (28)$$

The half opening displacement δ at the crack tip $x_1 = a$ becomes

$$\delta = \frac{8(1-\nu^2)\sigma_0 a}{\pi E}\left[\ln\frac{c}{a} - \frac{\sqrt{c^2-a^2}}{a}\left(\cos^{-1}\frac{a}{c} - \frac{\pi\sigma_\infty}{2\sigma_0}\right)\right] \quad (29)$$

The end of the macro-crack is fitted with a variable angle sharp wedge displayed in Fig. 9 where the length d<<b. The geometric shape of the macro-crack front via the mesoscopic zone is made compatible to the wedge. This gives

$$\delta^*(c,d) = d\tan\beta \quad (30)$$

Making use of eq. (27), there results:

$$\delta^*(c,d) = \mathrm{COD}\big|_{x_1=c-d} \quad (31)$$

Eqs.(30) and (31) may be combined to yield the second relation in addition to eq. (26) for solving the two unknowns band d.

5. Strain energy density function and scale shifting criterion criterion.

Even though the dual stress field solution provides the necessary requirement for distinguishing damage at the macroscopic and microscopic scale, it is not sufficient to determine when a given state of damage would shift from one scale to another. A criterion will be needed. To this end, use will be made of the volume energy density given by

$$\frac{dW}{dV} = (\frac{dW}{dV})_v + (\frac{dW}{dV})_d \tag{32}$$

which for the case of linear elasticity dW/dV can be decomposed into two parts: one for dilatation and one for distortion. They are indicated, respectively, by the subscripts v and d. According to the energy density criterion of fracture, dilatation is assumed to determine the location and threshold of fracture while distortion to failure by shape change such as in yielding. This criterion has been tested for both brittle and ductile materials in addition to static, dynamic and cyclic loadings [23,24]. When dilatation dominates the component

$$(\frac{dW}{dV})_v = \frac{1-2\nu}{6E}(\sigma_{11}+\sigma_{22}+\sigma_{33})^2 \tag{33}$$

would be larger than

$$(\frac{dW}{dV})_d = \frac{1+\nu}{6E}[(\sigma_{11}-\sigma_{22})^2+(\sigma_{22}-\sigma_{33})^2+(\sigma_{33}-\sigma_{11})^2+6\sigma_{12}^2] \tag{34}$$

But in no cases eqs. (33) and (34) would differ by an order of magnitude. In other words, it is not justified to neglect one against the other as it is done in plasticity where only the equivalent stress enters into the yield criterion. For non-linear materials, the separation in eq. (32) is no longer valid. Dilatational and distortional effects can still be determined from the stationary values of the energy density function where the relative maxima and relative minima would correspond to the locations of dominance by shape change and volume change, respectively. An extensive discussion of this with reference to anisotropic and/or non-homogeneous materials can be found in [36]. For the present discussion, it is sufficient to use the results of linear elasticity.

5.1 Near field energy density functions: macroscopic and microscopic.

At a macroscopic distance from the crack front, the energy density function possesses a 1/r singularity as follows:

$$\left(\frac{dW}{dV}\right)^t = \frac{1}{16\pi\mu}(3-4\nu-\cos\theta)(1+\cos\theta)\frac{(K^t)^2}{r} \tag{35}$$

in which μ and ν are averaged over macroscopic size region. At a fixed distance from the crack front, it is also convenient to use the energy density factor

$$S = r\left(\frac{dW}{dV}\right)^t = \frac{1}{16\pi\mu}(3-4\nu-\cos\theta)(1+\cos\theta)(K^t)^2 \tag{36}$$

In such a case, S can be interpreted as the energy released by extending the crack by a macroscopic distance r. At a microscopic distance from the crack front, the volume energy density can be expressed as

$$\left(\frac{dW}{dV}\right)^w = \frac{1+\nu}{2E}\left[(\sigma_{11}^w)^2+(\sigma_{22}^w)^2-\nu(\sigma_{11}^w+\sigma_{22}^w)^2+2(\sigma_{12}^w)^2\right] \tag{37}$$

where E and ν would be averaged over a microscopic region although no difference in notation is made here. It is also possible to define a volume energy density factor S^w here as

$$\left(\frac{dW}{dV}\right)^w = \frac{S^w(r,\theta)}{r},\ r\to 0 \tag{38}$$

in which

$$S^w(r,\theta) = r^{2\lambda_1-1}S_{11}(\theta) \tag{39}$$

It can be shown from the work in [34] that

$$S_{11}(\theta)=\frac{1}{\pi\mu}\left(\frac{1}{2}\lambda_1 K^{w}\right)^2\{4(1-2\nu)\cos^2(\lambda_1-1)\theta+(\lambda_1-1)^2 + (\lambda_1\cos 2\alpha+\cos 2\lambda_1\alpha)[(\lambda_1\cos 2\alpha+\cos 2\lambda_1\alpha)-2(\lambda_1-1)\cos 2\theta]\} \tag{40}$$

The factor $S^{w}(r, \theta)$ within a micro-scale distance to the main crack is no longer independent of the distance r.

5.2 Scale invariant criterion.

Failure may not always occur gradually or smoothly, the transition may shift from micro to macro. A scale invariant criterion is therefore needed. Since the force or total energy is not affected by change in size, they can be regarded as the invariant quantities in the transition process. More specifically, the stress σ can be converted from the macroscale to the microscale by using force as the invariant. This leads to the simple relation

$$\frac{\sigma_{macro}}{\sigma_{micro}}=\frac{A_{micro}}{A_{macro}}\rightarrow\frac{MPa}{GPa}\rightarrow 10^{-3} \tag{41}$$

where A designates area. Since macro-stress and micro-stress differs by a factor of 10^3, it follows that $A_{macro}= 10^3 A_{micro}$. If the total energy is used as the scale invariant, then the ratio of the volume energy densities at the macroscale and microscale can be written as

$$\frac{\mathcal{W}_{macro}}{\mathcal{W}_{micro}}=\frac{A_{micro}\ell_{micro}}{A_{macro}\ell_{macro}} \tag{42}$$

where $\mathcal{W}$ stand for dW/dV. Alternatively, eq. (42) can be written as

$$m_{micro\rightarrow macro}\ \ell_{micro}\ \mathcal{W}_{micro}=\ell_{macro}\ \mathcal{W}_{macro} \tag{43}$$

For a homogeneous system, m = 1 and $\mathcal{W}$ versus ℓ is a perfect hyperbola so that eq. (43) is indeed true and has been used with success in fracture mechanics. For non-homogeneous systems especially when specimens are microns in size, m can be found analytically by defining the degree of system inhomogeneity, say for a group of polycrystals or dislocations, similar to the mean free path of electrons. The length could represent the distance between the local and global points of the stationary values of the energy density function which has been used to determine the prospective path of failure [24]. It depends on the loading, geometry and material. Eq. (43) is illustrated in Fig. 10 using the subscripts 1 and 2 instead of macro and micro and hence it may read as

$$m_{2\rightarrow 1}\ \ell_1\ \mathcal{W}_1=\ell_2\ \mathcal{W}_2 \tag{44}$$

for a process that goes from 2 to 1 or vice versa. Hence, scale shifting may be accomplished in succession in steps for a prescribed spectrum.

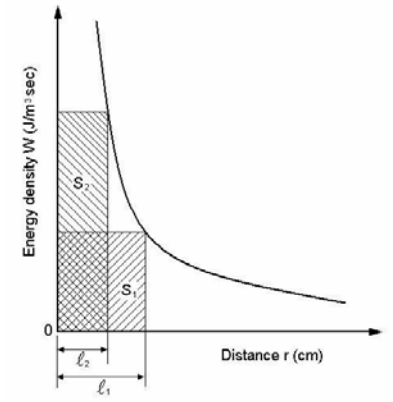

Fig. 10 Cross scaling criterion based on energy density versus distance relation

6. Discussion of numerical results.

Summarized in Tables 3 and 4 are the values of the length b for d = 0 of the single scale model and the length b and d for the dual scale model, respectively. It is more pertinent to show the openings of the macro-crack and micro-notch. They are denoted, respectively, by COD and RZOD in Fig. 11 for $\sigma_\infty/\sigma_o = 0.6$ computed by using the elastic properties of E = 200 GPa, $\nu = 0.3$ and $\sigma_o = 10$ MPa. All the curves decrease slowly at first and then more quickly when they approach the macro-crack tip $x_1 = a$ and the micro-notch tip $x_1 = c$ which are not the same for different β. Large β corresponds to blunter notch and the terminating locations of the curves tend to shift closer to $x_1 = a$. Note that the COD/a at the crack center has increased to 13×10^{-5} and maximum RZOD/a to 5.8×10^{-5}. More detailed information can be found in [18].

Similar to stress and strain, energy density is scale sensitive. When reference is made to a

Table 3. The values of the length b for different stress ratio σ_∞/σ_o for d = 0.

σ_∞/σ_o	0.1	0.2	0.3	0.4	0.5	0.6	0.7	0.8	0.9	1
b/a	0.0125	0.0515	0.1223	0.2361	0.4142	0.7013	1.2027	2.2360	5.3923	∞

Table 4. Values of lengths b and d for different angle β and stress ratio σ_∞/σ_o

β (deg.)		10	20	30	40	50	60	70	80
λ_1		0.500	0.503	0.512	0.530	0.563	0.616	0.6976	0.819
σ_∞/σ_o =0.1	b/a	0.0109	0.0108	0.0103	0.0119	0.0106	0.0091	0.0044	0.0002
	d/a×10^{-4}	0.4142	0.4428	0.6489	0.0238	0.1484	0.1638	0.2508	0.0144
σ_∞/σ_o =0.2	b/a	0.0463	0.0446	0.0442	0.0441	0.0412	0.0382	0.0253	0.0042
	d/a×10^{-4}	1.019	1.739	1.680	1.235	1.401	0.8404	0.8602	0.2100
σ_∞/σ_o =0.3	b/a	0.1080	0.1132	0.1167	0.1086	0.1010	0.1068	0.0806	0.0231
	d/a×10^{-4}	3.024	1.132	0.3501	1.629	2.424	0.3204	0.6448	0.4851
σ_∞/σ_o =0.4	b/a	0.2096	0.2273	0.2265	0.2046	0.2114	0.1906	0.1809	0.0726
	d/a×10^{-4}	4.611	0.4546	0.4530	4.092	1.268	1.906	0.3618	0.5082
σ_∞/σ_o =0.5	b/a	0.3602	0.3972	0.3834	0.3737	0.3678	0.3402	0.2980	0.1534
	d/a×10^{-4}	9.005	0.7944	2.300	2.990	2.207	2.381	1.192	0.6136
σ_∞/σ_o =0.6	b/a	0.6324	0.6377	0.6654	0.6590	0.6448	0.5877	0.5260	0.2624
	d/a×10^{-4}	6.324	5.102	1.331	1.318	1.290	2.351	1.052	1.050
σ_∞/σ_o =0.7	b/a	1.159	1.163	1.167	1.133	1.132	1.110	1.015	0.5894
	d/a× 0^{-4}	0.9272	0.6981	0.4670	1.359	0.6791	0.3331	0.2029	0.2358
σ_∞/σ_0 =0.8	b/a	2.112	2.177	2.171	2.128	2.103	2.009	1.747	0.9637
	d/a×10^{-4}	2.112	0.4354	0.4342	0.8511	0.6309	0.6028	0.5240	0.3855
σ_∞/σ_o =0.9	b/a	5.089	5.079	5.109	5.050	4.915	4.590	3.746	1.830
	d/a×10^{-4}	1.527	1.524	1.022	1.010	0.9831	0.9180	0.7492	0.3660

micro-volume of material, the apparent energy density will invariably be higher. To be more specific, dW/dV will be normalized with respect to σ_0^2/E and denoted by $\mathcal{W}^*$, i.e. $\mathcal{W}^* = E(dW/dV)/\sigma_0^2$, which will be plotted against the dimensionless distance r/a on the log-log scale. Numerical results are based on $\nu = 0.3$ and a half crack length of 10 mm. Since both the length of the restraining zone b and the length of the notch tip d are normalized to the same half crack length a, the data for b/a and d/a represent a true comparison of the macro and micro scale distance. Fig. 12 shows that variation of $\mathcal{W}^*$ with r/a for $\sigma_\infty/\sigma_o = 0.4$. Two sets of curves are obtained which appear as straight lines on a log-log plot. They are denoted by solid lines for $r^{-1/2}$ at a macro distance from the crack and solid circular dots at a micro distance $r^{\lambda_1 - 1}$ from the crack. The angle β takes the values of 20°, 50° and 80°. It is of interest to note that all the solid lines are parallel and they shift to higher energy density levels with increasing notch angle. All those line represented by circular dots tend to rotate counterclockwise with increasing β. The two sets of line give opposing effects for the energy density: one increases with β by translation and one decreases with β by rotation. The influence of the same microscopic defects is seen to give opposing effects when the scale level of observation is changed. Such a behavior has not been observed previously.

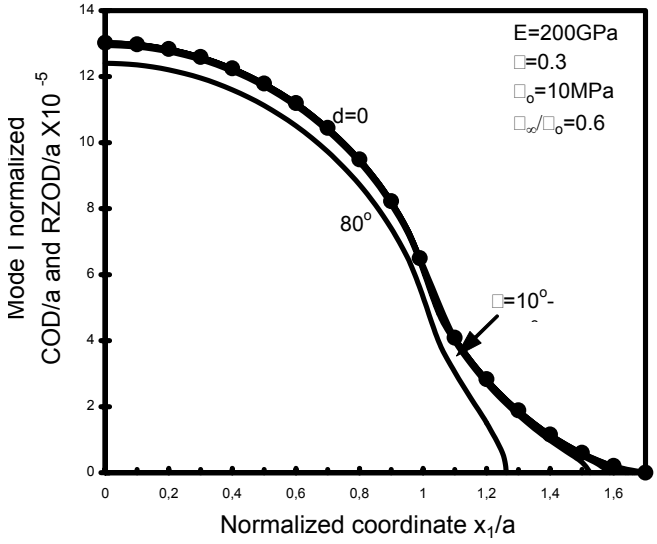

Fig. 11 Normalized COD/a and RZOD/a versus x_1/a for σ_∞/σ_o=0.6

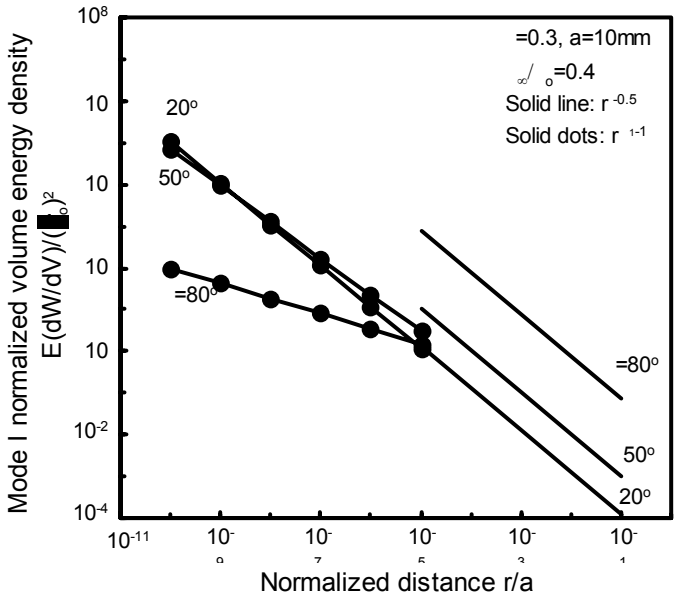

Fig. 12 Normalized energy density $E(dW/dV)/(\sigma_o)^2$ versus ratio r/a for σ_∞/σ_o=0.4

7. Conclusions and future work.

Fracture mechanics has been shying away from basic research for more than two decades with the hidden implication that new results might disturb the application of codes and standards that are made easy to apply for the industry. This need not be a concern anymore since the impact of electronics has shifted the emphases to the understanding of failure related to semiconductor surfaces and interfaces, an area that continuum mechanics thought that it could feel at home [5,6]. To the contrary, the new challenge brought out the weakness of the classical approach when applied to micron scales. There is little or no hope that the present approach could be applied to address the material damage process for microelectronics and macrostructures since this would require the reconciliation of the contrasting views of the continuum and the particulate [37,38] that have prevailed for centuries. It does not appear that this is the way to resolve the problem. On the other hand, it does appear justified to seek for new avenues of approach that should not be regarded as being provocative for those who wishes to follow traditions.

Despite the foregoing comments, it is worthwhile to learn from the results of some recent works showing that the state of affairs at the atomic and microscopic level can influence the macro-crack propagation behavior. Graphical display of results obtained from atomistic calculations [39] have revealed the presence of localized phonon-like modes near a moving crack tip, just prior to dislocation emission and crack branching events. Although these approaches provide additional motivation for research, equal amount of efforts should be placed on their relevancy to the macroscopic properties of the material. Embedding a Molecular Dynamic computational region around the crack tip [40,41] and applying micromechanics to the surrounding region have been attempted to develop a two-scale model in a single simulation. Uncertainties at the boundary of the two regions, however, make the outcome somewhat artificial. The model assumes that the continuum plasticity carck tip behavior should be recovered by the micromechanics approach. Such an apriori assumption may or may not hold. The fundamental problem of how to specify the nonequilibrium boundary conditions at the atomic and microscopic scale requires attention. Lacking in particular is a knowledge of the initial states of the material microstructure in terms of stress/strain or energy stored in the grain due to crystal nucleation and formation. The initial stresses and energies trapped in the material microstructure would no doubt have a first order effect on the creation of dislocations, microvoids, grain boundary imperfections, etc. The neglect of these initial conditions would leave any predictions in doubt, especially when the length scale of device are reduced to microns. Fundamentally speaking, this calls for a knowledge of the nonequilibrium behavior of crystals. Overflow of energy from one crystal to another deficient in energy cannot be addressed using equilibrium continuum mechanics theories because they assume the condition $\Delta V/\Delta A \rightarrow 0$ across a surface or interface. This is equivalent to disconnecting the interaction between surface and volume effects. To begin with, the classical approach assumes that the conditions on the surface or boundary are specified rather than determined. In addition, element size effect is made to vanish in all continuum mechanics theories. Stated more precisely:

Classical continuum mechanics is not intended to address conditions across any surface or interface; it specifies them as boundary conditions.

Computer simulation of atomic models would not describe the physical conditions across an interface since they pre-assumes the boundary conditions. Strictly speaking, there prevails only bi-phase problems where the conditions across an interface are derived as unknowns rather than specified as known quantities [19,20]. Representation of a continuous body by a discrete set of finite elements seems to lack justification if the procedure depends on the use of differential equations that were originally derived from a system with infinite number of elements. Such a fundamental discrepancy should not be overlooked, particularly when the approximate method is applied to solve for details near the local region around a crack. This is the reason why the singularity character of the solution must be embedded into the finite element method [26].

Mesofracture mechanics [42] is appealing as the discipline calls attention to the finiteness of the gap between any two arbitrary division of scaling. If the influence of geometry, loading and material type specified as a combination at the macroscopic scale can be felt at the scale level of investigation, it is then necessary to consider them in the model. If a singularity can uniquely represent the combined effect of geometry, loading and material for a specified scale, it is then capable to find a way to connect the different singularities using stress and opening displacement conditions for different scale size of defects or imperfections such as cracks and dislocations. This possibility has been shown for a dual

scale system of a macro-crack and micro-notch where use was made of the series of singularities of orders weaker than $r^{-1/2}$ that has been associated with a free crack surface at the macroscopic scale level. There also prevails a series of singularities stronger than $r^{-1/2}$; they may represent defects whose surfaces may not be traction free. Tractions may be present to restrain the surfaces from opening owing to the action of applied loads. These restraining stresses will again change with the geometry and material. By establishing the results of two succeeding singularity models, it might be possible to extend the range of scaling for a system that undergoes several transitions where each transition would correspond to a change in the degree of homogeneity described by a characteristic length parameter. These ideas are at their early stages of development. They are offered in the interest of research. If the answer is already known, then it would no longer be regarded as research and even less original.

Acknowledgement

The author wishes to express his gratitude to the Italian Group of Fracture (IGF) for the invitation to write this article and to present a lecture at the meeting in Bologna, Italy, June 16-18, 2004. The selection of the location cannot be more appropriate as it was the region near which scientific discoveries were made some 400 years ago. This fact lends to the opportunity of dedicating this article to the free spirit of the immortal Italian scientist Galileo Galilei in defiance of intimidation against the advancement of science. Indebted to in particular is Professor Alberto Carpinteri, Chairman of ICF 11, who will make this article available to the participants of ICF 11, March 20-25, 2005, Turin, Italy.

References

[1] D. S. Pan, C. C. Yang, C. F. Jou and B. Jogai, in: Pro. Workshop on Physics of Submicron Structures, Univ. of Illinois, (1982).

[2] R. S. Bauer (Ed.), in: Surface and Interfaces: Physics and Electronics, North Holland Physics Publishing, (1983).

[3] ASME Boiler and Pressure Vessel Code, Sec III, Appendix G, Nuclear Power Plant Components, American Society of Mechanical Engineers, New York (1980).

[4] ASME Boiler and Pressure Vessel Code, Sec. XI, Appendix A, Rules for In-Service Inspection of Nuclear Power Plant Components, American Society of Mechanical Engineers, New York (1980).

[5] Application of Fracture Mechanics in Electronic Package and Materials, T.Y. Wu, W.T. Chen, R.A. Pearson and D.T. Read, eds., ASME Electrical and Electronic Package and Applied Mechanics Division, EEP Vol.11 and AMD-Vol.64, New York (1995)

[6] Application of Fracture Mechanics in Electronic Package, W.T. Chen and D.T. Read, eds., ASME Applied Mechanics Division and Electrical and Electronic Package Division, AMD-Vol.222 & EEP-Vol.20, New York (1997)

[7] Plane strain crack toughness testing of high strength metallic materials, ASTM Special Technical Publication 410 (1996).

[8] G. C. Sih and C. Chen, Non-self-similar crack growth in an elastic-plastic finite thickness plate, J. of Theoretical and Applied Fracture Mechanics, 3(2) (1985) 125-139.

[9] G.C. Sih, Fracture Mechanics of engineering structural components, Fracture Mechanics Methodology, G.C. Sih and L. Faria, eds., Martinus, Nijhoff Publishers (Now Kluwer Academic Publishers, Boston) (1984) 35-101.

[10] G.C. Sih, Some basic problems in fracture mechanics and new concepts, J. of Engineering Fracture Mechanics, 5(2) (1973) 365-377.

[11] G. C. Sih, Mechanics of subcritical crack growth, in: G. C. Sih, N. E. Ryan and R. Jones, Fracture Mechanics Technology Applied to Evaluation and Structure Design, Martinus Nijhoff Publishers, The Netherlands (1982) 3-18.

[12] J. R. Rice, A path independent integral and the approximate analysis of strain concentration by notches and cracks, J. of Applied Mechanics, 35 (1968) 379-386.

[13] K. Niihara, New design concept of structural ceramics-ceramic nanocomposites, The Centennial Issue of the Ceramic Society of Japan, Journal of Society of Ceramic Society of Japan, 99(10) (1991) 974-982.

[14] K. Niihara, N. Onal and A. Nakahira, Mechanical properties pf (Y-TZP)-alumina-silicon carbide nanocomposites and the phase stability of Y-TZP particles in it, J. of Materials Science, 29 (1994)

164-168.
[15] J. H. Zhao, L. C. Stearns, M. P. Harmer, H. M. Chan and G. A. Miller, Mechanical behavior of alumina-silicon carbide nanocomposites, J. American Ceramic Society, 76(2) (1993) 503-510.
[16] G. R. Anstis, P. Chantikul, B. R. Lawn and D. B. Marshall, A critical evaluation of indentation techniques for measuring fracture toughness： Part I - Direct crack measurements, J. American Society of Ceramics, 64 (1981) 533-538 and P. Chantikul, G. R. Anstis, B. R. Lawn and D. B. Marshall, Part II -.Strength method, J. American Society of Ceramics, 64 (1981) 539-543
[17] K. Niihara, R. Morena and D. P. H. Hasselman, J. Materials Science letter 1 (1982) 13.
[18] G. C. Sih and X. S. Tang, Singularity representation of multiscale damage due to inhomogeneity with mesomechanics consideration, G. C. Sih, T. Kermanidis and Sp. Pantelakis, eds., Sarantidis Publications, Patras, Greece (2004) 1-15.
[19] G.C. Sih, Thermomechanics of solids: nonequilibrium and irreversibility, J. of Theoretical and Applied Fracture Mechanics, 9(3) (1988) 175-198.
[20] G.C. Sih, Some basic problems in nonequilibrium thermomechanics, S. Sienietyez and P. Salamon, eds., Tayler and Francis, New York, (1992) 218-247.
[21] W. E. Anderson and R. A. Davis, A view of Boeing- Lehigh activities in LEFM and some consequences, in: G. C. Sih, R. P. Wei and F. Erdogan (Eds.), Linear Fracture Mechanics: historical development and Application of LEFM, Envo Publishing Co., Bethlehem, PA (1974) 41-56.
[22] Linear Fracture Mechanics: historical development and Application of LEFM, G. C. Sih, R. P. Wei and F. Erdogan (Eds.), Envo Publishing Co., Bethlehem, PA (1974).
[23] G.C. Sih, The role of surface and volume energy in the mechanisms of fracture, in: V. Balakrishnan and E. E. Bottani, Mechanical Properties of Solids: Plastic Instabilities, World Scientific, Singapore, (1985) 396-461.
[24] [24] G.C. Sih, Mechanics of fracture initiation and propagation, Kluwer Academic Publishers, The Netherlands, 1991.
[25] G.C. Sih and D.Y. Tzou, Plastic deformation and crack growth behavior, Plasticity and Failure Behavior of Solids, G.C. Sih, A.T. Ishlinsky and S.T. Mileiko, eds., Martinus, Nijhoff Publishers (Now Kluwer Academic Publishers, Boston) (1990) 91-114.
[26] P. D. Hilton and G. C. Sih, Application of the finite element method to the calculation of stress intensity factors, in: G. C. Sih (Ed.), Method of Analysis and Solutions of Crack Problems, Noordhoff International Publishing, Leyden, 1 (1973) 426-515.
[27] G. C. Sih, Mechanics and physics of energy density and rate of change of volume with surface, J. of Theoretical and Applied Fracture Mechanics, 4(3) (1985) 157-173.
[28] G. C. Sih, Survive with the time o'clock of nature, G. C. Sih and L.Nobile, eds., Tipografia Moderna, Bologna, Italy (2004) 1-18.
[29] K.J. Cheng and S.Y. Cheng, Boundary conditions of electrons at interface: Part I – Mixture of nanometer crystals and amorphous silicon and Part II- Internal stresses in thin films, in: G. C.Sih and V.E. Panin, (eds.), Prospects of Mesomechanics in the 21th century, J. of Theoretical and Applied Fracture Mechanics, 37 (2001) 11-27.
[30] G. C. Sih, Crack propagation characteristics trespassing the Rayleigh wave speed barrier as influenced by applied stress and velocity dependent local zone of restrain, J. of Theoretical and Applied Fracture Mechanics, 41 (2004) 185-231
[31] S. M. Ohr, An electron microscope study of crack tips deformation and its impact on the dislocation theory of fracture, Material Science Engineering, 72 (1985) 1-35.
[32] G. P. Cherepanov, Mechanics of Brittle Fracture, McGraw-Hill, New York, (1979).
[33] G. I. Barenblatt, Concerning equilibrium cracks forming during brittle fracture: the stability of isolated cracks, relation with energetic theories, Applied Mathematics and Mechanics (PMM) 23 (1959) 1273-1282.
[34] D. C. Dugdale, Yielding of steel sheets containing slits, Journal of the Mechanics and Physics of Solids, 8 (1960) 100-104.
[35] G.C. Sih and J.W. Ho, Sharp notch fracture strength characterized by critical energy density, J. of Theoretical and Applied Fracture Mechanics, 16(3) (1991) 179-214.
[36] G. C. Sih and E.P. Chen, Dilatational and distortional behavior of cracks in magnetoelectroelastic materials J. of Theoretical and Applied Fracture Mechanics, 39(3), (2003) 1-21.

[37] G. C. Sih, Implication of scaling hierarchy associated with nonequilibrium: filed and particulate, J. of Theoretical and Applied Fracture Mechanics, 37(3) (2001) 335-369. 175-198.
[38] G.C. Sih, B. Liu (2002), Mesofracture mechanics: a necessary link, Prospects of Mesomechanics in the 21st century, G.C. Sih and V.E. Panin, eds., Special issue of J. of Theoretical and Applied Fracture Mechanics, 37, 335-36.
[39] B.L. Holian, S.J. Zhou, P.S. Lomdahl, N. Gronbech-Jensen, D.M. Beazley and R. Ravelo, Molecular-dynamics simulation of fracture: an overview of system size and other effects, Mat. Res. Soc. Symp. Proc., 409(1996)3-9.
[40] H. Noguchi and Y. Furuya, A method of seamlessly combining a crack tip molecular dynamics enclave with a linear elastic outer domain in simulating elastic-plastic crack advance, International Journal of Fracture, 87(1997) 309-329.
[41] Y. Furuya, H. Noguchi, A combined method of molecular dynamics with micromechanics improved by moving the molecular dynamics region successively in the simulation of elastic-plastic crack propagation, International Journal of Fracture, 94 (1998) 17-31.
[42] Mesofracture Mechanics, in: G. C. Sih (ed.), Current Approaches to Material Damage at Different Size and Time Scales, J. of Theoretical and Applied Fracture Mechanics, 41 (2004).